# Extensor-Based Image Interpolation

*Kannappan Palaniappan* *Jeffrey Uhlmann* *Dong Li*

Multimedia Communication and Visualization Laboratory
Department of Computer Engineering and Computer Science
University of Missouri, Columbia, MO 65211, USA
Email: {palani, uhlmann}@cecs.missouri.edu, dl17b@mizzou.edu

**ABSTRACT**

We propose a novel image interpolation method for resolution enhancement of still images. The approach consists of a nonlinear mapping from pixel index space to color space based on the low-resolution image so that non-integral pixel indices in a super-sampling can be mapped to colors, i.e., interpolated. This nonlinear mapping is based on an extensor transformation of 2D pixel indices to an *N*-dimensional vector space that encodes the Euclidean proximity interrelationships among a neighborhood of *N* pixels. Experimental results indicate that extensor-based interpolation yields results that are qualitatively superior to classical bilinear and bicubic interpolation, that has important advantages in comparison to edge-directed [4] and optimal-recovery [10] interpolation methods, and that has comparable or lower computational cost.

## 1. INTRODUCTION

Image interpolation and superresolution methods are used to produce higher-resolution images from one or more lower-resolution datasets. Common applications requiring image interpolation include image coding, image reconstruction, enlarging photographs, image repairing or flaw correction, and transcoding NTSC video content to higher spatial or temporal resolution formats like HDTV.

Models of image interpolation, which have been extensively studied, can be broadly divided into two approaches, linear and nonlinear. Classical linear interpolation techniques such as nearest neighbor, bilinear, bicubic and bicubic spline interpolation [2] are computationally efficient but tend to blur edges and introduce aliasing artifacts. Partial differential equation, variational and directional interpolation methods [1, 3] are much more sophisticated and yield qualitatively superior results. The major disadvantage of these methods is their substantially higher computational cost.

Recent work in the area of image interpolation has emphasized the need to develop methods that yield superior perceptual image quality and computational efficiency. Edge-directed interpolation introduced covariance-based adaptation, which exploits maintaining a correspondence between interpolated high-resolution and measured low-resolution local covariance structure [4]. Example-based interpolation algorithms employ a database of training images to create plausible high-frequency details in zoomed images [5]. Rather than making assumptions about the continuity of the underlying signal and its derivatives as in the common image interpolation methods, the wavelet-based interpolation methods compute a measure of local regularity and preserve this local regularity in the interpolated image [6, 7]. Some neural network algorithms such as radial basis functions, self-organizing feature maps, Markov trees and Generalized Regression Neural Networks [8, 9, 5] are employed to improve the image quality through kernel-based methods. These newer interpolation algorithms attempt to improve perceptual visual quality by reducing artifacts and enhancing details like sharpening edges.

## 2. EXTENSOR-BASED INTERPOLATION

We propose a novel extensor-based image interpolation scheme in this paper. Our approach is based on the idea that there is a non-linear mapping or relationship between a measured set of parameters such as color and the lifted-distances among pixels. We estimate the high-resolution interpolated value from a low-resolution counterpart with a qualitative model characterizing the relationship between the intensities and the lifted-distances.

Functions that lift a *d*-dimensional vector into a superspace of *N* dimensions will be referred to as *extensor functions*, and the *N*-dimensional vectors as *extensors*. A suitable choice of extensor functions determines the interpolant properties. Suppose the d-dimensional extensor neighborhood (i.e. $d$=2 for images, $d$=3 for video), $S$, contains N pixels. It is preferable to define extensor functions with certain desirable properties under certain classes of transformations. For example, given an extensor function $f$ and a linear transformation **L**,

the extensor defined by a pixel index vector **x** should satisfy $f(\mathbf{Lx}) = \mathbf{L}f(\mathbf{x})$. However, extensor functions exhibiting a similar property for restricted classes of transformations (e.g., scale and rotation) may be just as satisfactory with respect to a human visual quality assessment of the resulting interpolation.

One well-known class of extensor functions uses products of subsets of index values. For example, if the index values for an image pixel to be interpolated are $u$ and $v$, then a possible rank 6 extensor would use $[u^2, v^2, uv, u, v, 1]$, or for a rank 10 extensor, $[u^3, v^3, u^2v, v^2u, u^2, v^2, uv, u, v, 1]$. This class of extensors defines polynomial reproduction. However, high order polynomial interpolations tend to exhibit undesirable oscillatory characteristics and have sufficient rank for a relatively small set $S$.

The extensor defined using an Euclidean norm function that encodes all pairwise distances between pixels within a specified neighborhood is constructed as shown in Eq (1). The column $j$ of the extensor matrix is defined by the indices of pixel $i$ in set $S$ of $N$ pixels in $d$-dimensions via a nonlinear mapping, $Ext(X_j)$.

$$\mathcal{X} = \frac{1}{K}\begin{bmatrix} \varphi_{11} & \varphi_{12} & \cdots & \varphi_{1N} \\ \varphi_{21} & \varphi_{22} & \cdots & \varphi_{2N} \\ \vdots & \vdots & \vdots & \vdots \\ \varphi_{N1} & \varphi_{N2} & \cdots & \varphi_{NN} \end{bmatrix} \quad (1)$$

where $\varphi_{ij} = h(X_i - X_j) = \|X_i - X_j\|$, i,j = 1,2, ...., N (2)

$\|\bullet\|$ denotes a norm usually Euclidean (or 2-norm), $X_1$, $X_2$, …, $X_N$ are distinct spatial locations of known pixels, or measurements in $d$-dimensions and $K$ is a normalization factor based on the scale of the interpolation (i.e. $K = 2$ when the image size is doubled). Each column of Eq 1 is an extensor function, with the notation $Ext(y)$ denoting the extensor vector for pixel $y$,

$$Ext(y) = \begin{bmatrix} \|X_1 - y\| \\ \|X_2 - y\| \\ \vdots \\ \|X_N - y\| \end{bmatrix} \quad (3)$$

The signal space $\tilde{G}$ is $g$-dimensional, $g$=3 for color intensities. The transformation mapping from the distance or index-based extensor matrix, $\mathcal{X}$, to the color matrix $\tilde{G}$, is defined using an interpolation matrix as,

$$T_{3\times N}\mathcal{X}_{N\times N} = \tilde{G}_{3\times N} \quad (4)$$

We need to solve for the multidimensional (i.e. color intensity) extensor interpolating matrix $T_{3\times N}$ under the Euclidean distance projection. The Euclidean distance matrix using Eq 1 and 2 is guaranteed to be positive definite and hence invertible [11]. The columns of $\tilde{G}$ are feature values such as multispectral color, pressure, temperature, velocity, voltage, current, etc. Subsequently, any other arbitrary index vector $y$ with extensor function $Ext(y)$ has associated color vector $T\,Ext(y)$. Given a non-singular extensor matrix, $\mathcal{X}$, $T$ can be determined as

$$T_{3\times N} = \tilde{G}_{3\times N}\mathcal{X}^{-1}_{N\times N} \quad (5)$$

and this transformation used to interpolate (or even extrapolate) color vectors for pixels between (or outside of) the pixels within the region $S$. The matrix $\tilde{\mathrm{G}} = [\vec{\tilde{\mathrm{G}}}_1\ \vec{\tilde{\mathrm{G}}}_2\ ...\ \vec{\tilde{\mathrm{G}}}_\mathrm{N}]_{3\times\mathrm{N}}$, where $\vec{\tilde{G}}_j$ is the mean corrected $g$-dimensional measured column vector (i.e. three spectral measurements such as rgb) associated with extensor $X_j$. Mean correction ensures that constant image regions (zero mean) are interpolated without bias, hence

$$\begin{aligned} \tilde{G}_{3\times N} &= [\vec{G}_1 - \vec{\mu}_G\ \vec{G}_2 - \vec{\mu}_G\ \cdots \vec{G}_N - \vec{\mu}_G]_{3\times N} \\ &= G_{3\times\mathrm{N}} - [\vec{\mu}_G]_{3\times 1}[1\ 1\ \cdots 1]_{1\times N} \end{aligned} \quad (6)$$

where $\mu_G$ is the mean (average) color intensity of the pixels within the local extensor neighborhood, S.

We determine the color intensities for the interpolated pixel using

$$\vec{G}(y) = T \cdot Ext(y) = \tilde{G}\mathcal{X}^{-1}Ext(y) + \vec{\mu}_G \quad (7)$$

where $y$ denotes the (non-integer) location of the pixel for which color interpolation is desired, and $Ext(y)$ is the extensor vector for the interpolation pixel position $y$.

## 3. EXPERIMENTAL RESULTS

We qualitatively compare the extensor-based interpolation with bilinear, bicubic [2], edge-directed [4] and optimal-recovery methods [10]; the latter two methods were Matlab implementations directly provided by the original authors on their web sites. The original 512x512 Lena Sjööblom 1972 image shown in Fig 1a is subsampled to a 256x256 image; the decimated image is derived from the even rows and columns of the original image. We depend on subjective evaluation to assess the visual quality of the interpolated images. The extensor neighborhood, $S$ are non-overlapping rectangular domains of size 7x7 with N=49 to implement the interpolation. On a good quality color monitor the variation in visual quality can be readily discerned from a normal viewing distance. Figures 2(a) and (b) show a zoom factor of two applied to the face subregion of the subsampled image. The extensor method performs similar to the edge-directed and optimal recovery interpolations. However, zooming-in reveals further differences. For example, the hat subregion (Fig 3a) is interpolated with some circulatory artifacts by the edge-directed and optimal-recovery methods at a scale factor of 4 in Fig 3e and 3f. Finally, zooming in by a factor of 8 in the eye region, Fig 4a-4g, show that the extensor method

preserves the circular features of the iris and small structures of the eye brow better than other methods. The edge-redirected and optimal interpolation methods introduce significant artifacts at the higher resolution that appear to derive from the spurious enhancement of short, edge-like structures which exist at the natural resolution limits of the original image. In other words, the edge-enhancement feature of [4] succeeds in maintaining the appearance of edge structures, but at the cost of distorting the sharp circular discontinuities at increasing super-resolutions. The extensor-based interpolation provides equivalent or superior perceptual quality at reduced computation cost especially at high zoom factors.

## 4. REFERENCES


[1] M. Bertalmio, G. Sapiro, V. Caselles, C. Ballester, "Image inpainting", Proc ACM SIGGRAPH, pp. 417-424. July 2000

[2] A.K. Jain, Fundamentals of Digital Image Processing, Prentice-Hall 1988

[3] H. Chen, G.E. Ford "Image interpolation by inhomogeneous diffusion", Proc. IEEE Int. Conf. Image Processing, pp. 581-585, 1994.

[4] X. Li and M.T. Orchard, "New edge-directed interpolation", IEEE Transactions on Image Processing, 10(10): 1521-1527, Oct. 2001. http://www.ee.princeton.edu/~lixin

[5] W.T. Freeman, T.R. Jones, E.C.pasztor, "Example-based super-resolution", IEEE Computer Graphics and Applications, pp. 56-65 March/April 2002.

[6] W.K. Carey, D.B. Chuang, S.S.Hemami, "Regularity-preserving image interpolation", Proc. IEEE Int. Conf. Image Processing, Volume 1, pp 901-904 1997.

[7] D.D. Muresan and T.W. Parks, "Image interpolation using wavelet-based hidden markov trees", IEEE ICASSP, pp2304-2307, 2001.

[8] F.M. Candocia and J.C. Principe. "Super-resolution of images based on local correlations". IEEE Trans Neural Networks, 10(2): 372-380, Mar. 1999.

[9] M.P. Wachowiak, A.S. Elmaghraby, R. Smolikova, J. M.Zurada "Generalized regression neural networks for biomedical image interpolation" Proc. INNS-IEEE Joint Conf Neural Networks, pp 2133-2138, 2001.

[10] D.D. Muresan T.W. Parks, "Adaptive, optimal-recovery image interpolation", IEEE ICASSP, pp. 2297-2300, http://dsplab.ece.cornell.edu/software/interploation, 2001

[11] I.J. Schoneberg, "Metric spaces and completely monotone functions", Annals of Math, 39:811-841, 1938.


Figure 1 Original Image (512 by 512)


Figure 2a Optimal-recovery 2x


Figure 2b Extensor-Based (7-by-7) 2x


Figure 3a Subsampled hat

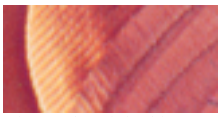
Figure 3b Original image (Hat)


Figure 3c Bilinear 4x


Figure 3d Bicubic 4x

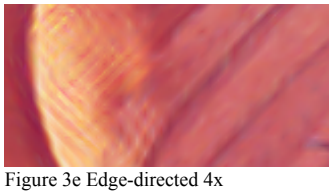
Figure 3e Edge-directed 4x

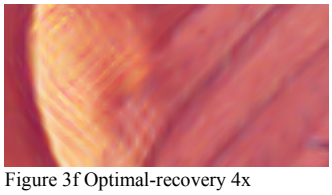
Figure 3f Optimal-recovery 4x

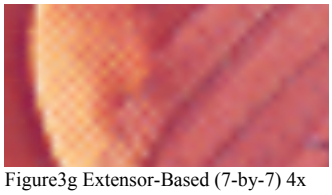
Figure3g Extensor-Based (7-by-7) 4x

Figure 4a Subsampled image (Eyes)

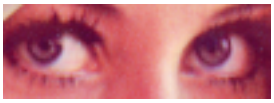

Figure 4b Original image (Eyes)

Figure 4c Bilinear 8x

Figure 4d Bicubic 8x

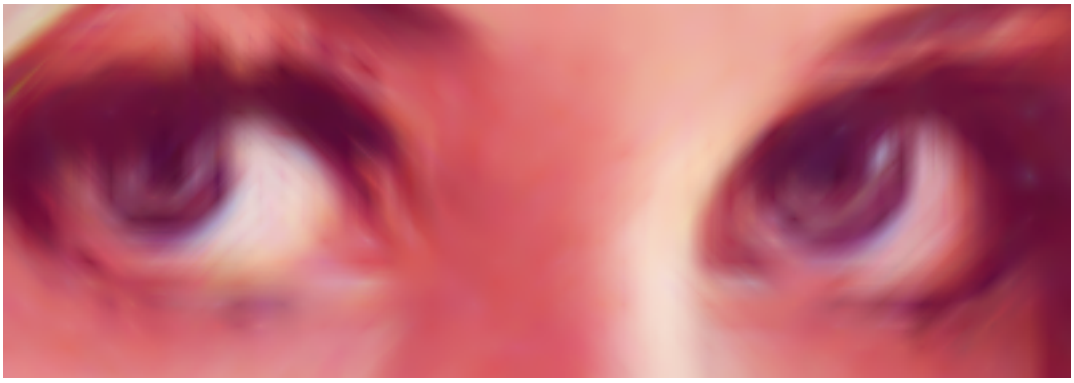

Figure 4e Edge-directed 8x

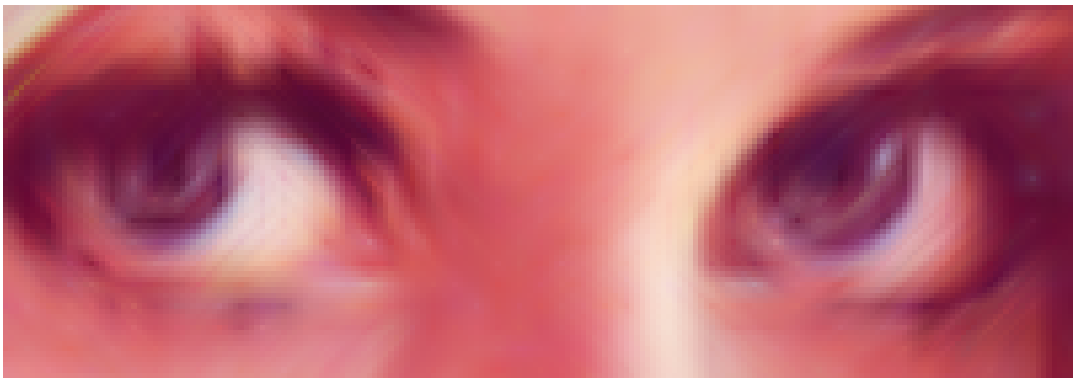

Figure 4f Optimal-recovery 8x

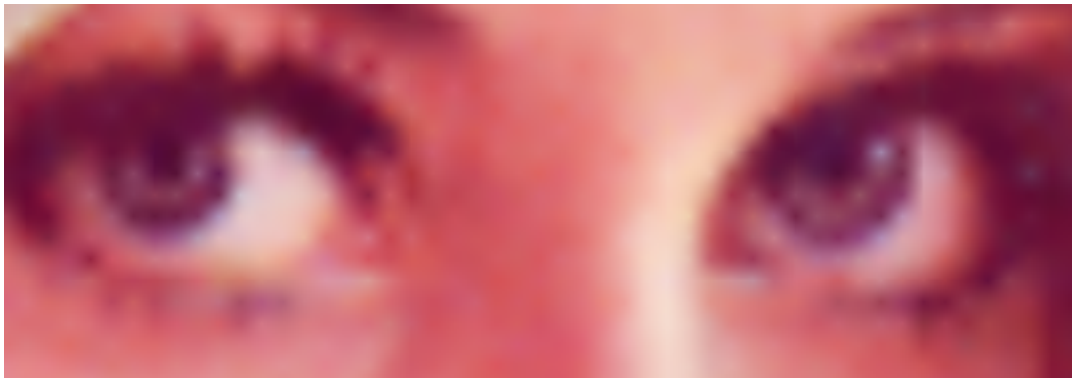

Figure 4g Extensor-based 8x